

THERMAL INERTIA AND THERMAL CONDUCTIVITY MEASUREMENTS OF WELL-CHARACTERIZED MARS ANALOG ROCKS. A. A. Ahern¹, A. D. Rogers¹, R. J. Macke², B. J. Thomson³, R. Kronyak⁴, G. Peters⁴, E. Carey⁴. ¹Stony Brook University Department of Geosciences, Earth and Space Science Building, Stony Brook, NY 11767 (alexandra.ahern@stonybrook.edu). ²Vatican Observatory, V-00120, Vatican City State. ³Dept of Earth & Planetary Sciences, Univ. of Tennessee Knoxville, Knoxville, TN 37996. ⁴NASA Jet Propulsion Laboratory, Pasadena, CA 91109.

Introduction: Mars surface rocks have diverse physical and chemical properties, as observed in orbiter and rover imaging and characterization. The physical properties (e.g., grain size, induration, cementation, porosity, vesicularity, etc.) of rocks can provide crucial information as to their petrogenetic origins and diagenetic histories.

Thermal inertia (I) is the intrinsic property of a material that describes how efficiently that material can absorb, conduct, and re-radiate heat. It is given by in eq. 1:

$$I = \sqrt{k\rho c}. \quad (\text{eq. 1})$$

Here, k is the bulk thermal conductivity (W/mK), ρ is the bulk density (kg/m³), and c is the specific heat capacity (J/kgK); I is given in units of Jm⁻²K⁻¹s^{-1/2}.

I has been widely used in planetary studies as a proxy for the physical characteristics of rocks and sediment (e.g., grain size, cementation quality, or porosity) of the near sub-surface (upper few cm) [1-3]. Orbital and rover-based observations have used surface temperatures derived from emissivity measurements over diurnal and seasonal cycles in an attempt to define the I , and thus, the physical nature, of the martian surface [4-10]. Studies described in [11-15] have also been conducted on geologic particulates to relate grain size, shape, density, and sorting to k values, these being the only studies done at Mars-relevant atmospheric pressures. Other work has been done to model the behavior of k of both consolidated and unconsolidated particles at martian pressures [16,17]. However, there are no comprehensive studies linking physical properties of Mars-relevant rocks with k values, and thus, I values at Mars atmospheric pressures. Some studies have reported I or k values of singular or small batches of rocks but methods and conditions between different lab setups vary greatly [18-20].

The goal of this work is to present a suite of well-characterized rock samples of known physical properties with k values, all measured in the same conditions. We explore the relationships of quantified physical properties (bulk density, porosity, uniaxial compressive strength) and chemical properties (bulk mineralogy, major element analyses) with thermal properties (I and k).

Methods: Samples used in this study represent the range of rock types observed or expected on the martian surface. These samples are summarized in Table 1. Grain density (ρ_g) measurements were done on each sample at the Vatican Observatory using a Quantachrome Ultrapycnometer 1000 ideal-gas pycnometer with gaseous nitrogen. Bulk density (ρ_b) measurements were also conducted at the Vatican Observatory with a NextEngine model 2020i Scanner HD Pro laser scanner and Geomagic Verify software. Porosity was then calculated according to:

$$P = 1 - \left(\frac{\rho_b}{\rho_g}\right). \quad (\text{eq. 2})$$

These values are reported in Table 1. Select samples were previously measured for uniaxial compressive strength (UCS) and were reported in studies [21-23] (Table 1).

Thermal measurements were conducted at Stony Brook University in the Vibrational Spectroscopy Lab using sensors produced by C-Therm Technologies. The rock measurements specifically used the C-Therm Modified Transient Plane Source (MTPS) and Flex Transient Plane Source (Flex TPS) sensors (Figure 1). These sensors use interfacial heat reflectance, i.e. the sensors supply known quantities of heat to the sample set against them, measure the drop in voltage as heat moves into the sample, and convert the change in voltage to thermal inertia values. The MTPS sits atop a metal cylinder, upon which the rock sample is placed. The Flex TPS is sandwiched between two discs of the rock sample and heat moves out of the top and bottom of the sensor. Measurements done with C-Therm equipment are non-destructive and sample preparation merely consists of cutting and polishing rocks to produce flat, smooth surfaces that sit flush against sensor planes. The largest challenges come in getting proper sensor-sample contact of grainy or friable samples and we expect errors from these samples to be higher than those with flatter or smoother surfaces.

Single measurements with C-Therm sensors take 90-150 s. This includes equilibrating, heating, and sampling. Sensors only heat by 1-3° C per measurement. Therefore, individual measurements are more energy and time-efficient, and simple to collect when compared with other methods that often require much more heating and equilibration time [e.g., 11-15,

18-20]. Due to these benefits, we are able to take many thermal measurements at a time to ensure reproducibility. In this study we have measured each rock sample in ambient P/T conditions 30 times (3 groups of 10 measurements per sensor contact). We also have measured each sample 15 times (3 groups of 5 per sensor contact) in 1 mbar increments between 1-10 mbar. Pressure is maintained within 0.1% of the set pressure using a Nor-Cal Intellisys IQ+ throttling butterfly valve. This was done in a glass vacuum cylinder at ambient T.

Results: The results of the thermal measurements at 1 bar and 6 mbar pressures compared with physical properties are given found in Table 1 & Figure 1. Work on links between chemical properties is still in progress.

Acknowledgments: This work was funded by the NASA PDART program, #80NSSC20K0548 to A. D. R.

References: [1] Wechsler, A.E. and Glaser, P.E. (1965) *Thermal Char. of the Moon*, 215-241. [2] Jakosky, B. (1986) *Icarus*, 66, 117-124. [3] Kieffer, H.H. et al. (1977) *JGR*, 82, 4249-4291. [4] Audouard, J. et al. (2014) *Icarus*, 233, 194-213. [5] Edwards, C.S. et al. (2018) *JGR*, 116(E10). [6] Fergason, R.L. et al. (2006) *JGR*, 111(E12004). [7] Putzig, N.E. et al. (2005) *Icarus*, 173, 325-341. [8] Putzig, N.E. and Mellon, M.T. (2007) *Icarus*, 191, 52-67. [9] Vasavada, A.R. et al. (2017) *Icarus*, 284, 372-376. [10] Mellon, M.T. et al. (2000) *Icarus*, 148, 437-455. [11,12] Presley, M.A. and Christensen, P.R. (1997a,b) *JGR*, 102, 6551-6566. [13] Presley, M.A. and Craddock, R.A. (2006) *JGR*, 111(E9). [14,15] Presley, M.A. and Christensen, P.R. (2010a,b) *JGR*, 115(E7). [16,17] Piqueux, S.R. and Christensen, P.R. (2009a,b) *JGR*, 114(E9). [18] Kahle, A. (1980) *Remote Sen. in Geol.*, 227-273. [19] Sass, J.H. et al. (1971) *JGR*, 76, 3391-3401. [20] Midtømme, K. and Roaldset, E. (1999) *Geol. Soc. London*, 158, 45-60. [21] Kronyak, R.E. et al. (2020) *ESS*, 7. [22] Thomson, B.J. et al. (2013) *JGR Planets*, 118, 1233-1244. [23] Panossian, L.T. et al. (2016) *LPSC XLVII*, Abstract #2949.

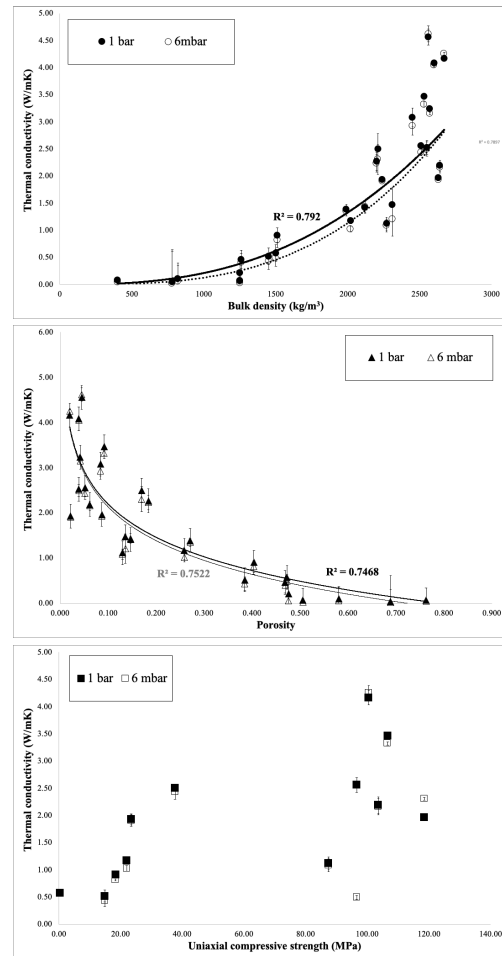


Figure 1: Rock conductivity measurements compared with bulk density (top), porosity (middle), and UCS (bottom) from rocks in Table 1. Closed and open shapes represent measurements at pressures of 1 bar and 6 mbar, respectively. Horizontal error bars in all of the plots are smaller than the data point size. As qualitatively expected, larger ρ_b and smaller porosity values result in higher k values. However, since porosity is a function of both ρ_b and ρ_g and ρ_g is affected by compositional variation, we cannot fully predict porosity with k .

Table 1. Summary of samples and their measured properties used in this study.

Sample Code	Sample Name	Sample Locality	Description	ρ_s (kg/m ³)	ρ_b (kg/m ³)	Porosity*	Mean UCS (MPa)	k (W/mK) @ 1 bar	k (W/mK) @ 6 mbar	k error
BAS-02	n/a	Keeler, CA	Vesicular basalt	2610	2270	0.130	87.45	1.1218	1.0851	0.117
BAS-ANT	n/a	Carapace Nunatak, ANT	Basaltic sandstone	2480	2120	0.147	n/a	1.4173	1.4352	0.106
BTL-049	Bishop Tuff-Intermediate	Bishop, CA	Rhyolitic welded tuff	2350	1450	0.385	14.90	0.5199	0.4332	0.152
C-SH	n/a	St. Clair, PA	Carbonaceous shale	2650	2550	0.039	n/a	2.5264	2.4977	0.129
CL-3	Clinch Formation	Knoxville, TN	Quartzose sandstone	2810	2640	0.062	103.57	2.1919	2.1604	0.102
CR-2	Chapman Ridge Fm	Knoxville, TN	Fine-grained calcareous sandstone	2720	2670	0.020	100.48	4.1663	4.2562	0.028
CRG-025-2	China Ranch Gypsum	Pahrump, NV	Gypsum	2290	2240	0.022	23.50	1.9307	1.906	0.019
CU-4	Cutler Formation	Paradox Basin, UT	Arkosic sandstone	2780	2530	0.092	106.63	3.4667	3.3239	0.051
JU-2	Juniper Formation	Knoxville, TN	Siltstone	2700	2600	0.039	n/a	4.086	4.0492	0.037
KAL-01-005	n/a	Mammoth Mountain, CA	Kaolinite	2540	1510	0.404	18.38	0.9107	0.8154	0.135
LRB-001-2	Lower Ridge Basin	Ridge Basin, CA	Fine-grained sandstone	2680	2570	0.042	n/a	3.2376	3.1543	0.022
LS-01	n/a	Santa Barbara, CA	Fine-grained limestone	2730	2020	0.259	22.00	1.1754	1.2039	0.055
MIS-2	Missoula Mudstone	Missoula, MT	Bentinitic mudstone	2840	1500	0.473	0.37	0.5756	0.4934	0.156
MO-3	Morrison Formation	eastern UT/western CO	Sandstone	2680	2560	0.045	n/a	4.5621	4.6221	0.149
MRB-001-1	Middle Ridge Basin	Ridge Basin, CA	Sandstone	2670	2310	0.136	n/a	1.4741	1.2098	0.320
MRB-001-2	Middle Ridge Basin	Ridge Basin, CA	Sandstone	2690	2200	0.184	n/a	2.2723	2.2334	0.163
NBS-022	Napa Basaltic Sandstone	Napa Valley, CA	Basaltic sandstone	2650	2510	0.052	96.60	2.5623	2.4346	0.056
ODP-031-1	Old Dutch Pumice	Ridgecrest, CA	Fine grained ashfall	2380	1250	0.476	n/a	0.2183	0.0570	0.161
Pumice-ADR	n/a	n/a	Pumice	1710	400	0.763	n/a	0.0772	0.0448	0.041
Puna 1	Campos de Piedra Pomez Ignimbrite	Campos de Piedra Pomez, ARG	Rhyolitic ignimbrite	2530	1250	0.506	n/a	0.0691	0.0249	0.080
Puna 3	n/a	Campos de Piedra Pomez, ARG	Ignimbrite	2370	1260	0.469	n/a	0.4638	0.4047	0.172
Puna 4	n/a	Campos de Piedra Pomez, ARG	Fine lapilli tuff	2500	780	0.689	n/a	0.0468	0.0194	0.596
Puna 5	n/a	Campos de Piedra Pomez, ARG	Pumice-rich tuff	1960	820	0.581	n/a	0.1054	0.0602	0.295
SILT-CA	n/a	n/a	Siltstone	2680	2450	0.084	n/a	3.0839	2.9254	0.173
SS-01	n/a	St. George, UT	Quartz arenite	2660	2210	0.170	37.70	2.5033	2.9627	0.275
USB-048-1	Uniform Saddleback Basalt	Boron, CA	Aphanitic basalt	2890	2630	0.087	118.50	1.9681	1.9296	0.013
WI-2	Wingate Formation	southeastern UT	Red eolian sandstone	2720	1990	0.271	n/a	1.3906	1.3502	0.086

*Average errors: $\rho_s = 17 \text{ kg/m}^3$, $\rho_b = 8 \text{ kg/m}^3$, porosity = 0.007